



# UPDATE ON THE ANALYSIS OF GSI2 AND GSI1 $^{16}\text{O}$ (200 MeV)

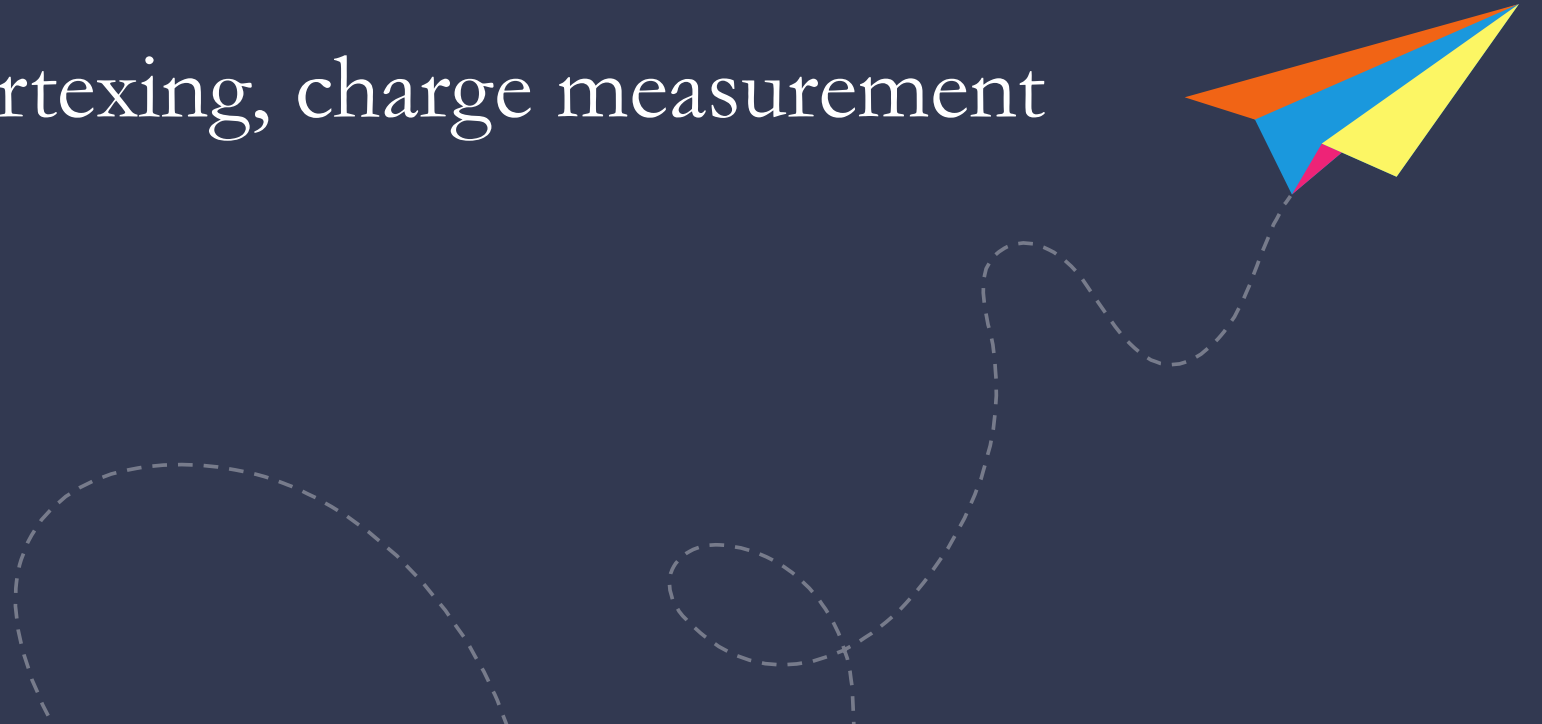
A. Alexandrov, A. Di Crescenzo, G. De Lellis, G. Galati, V. Gentile,  
A. Iuliano, A. Lauria, M.C. Montesi, A. Pastore, V. Tioukov

*Università di Napoli “Federico II”, INFN Napoli*  
*Università di Bari “Aldo Moro”, INFN Bari*

Physics Meeting, ZOOM, 07/04/2021

# Outline

- Status of the paper submitted on OPEN PHYSICS
- Status of the analysis
  - Scanning Progresses
  - GSI1: tracking, vertexing, charge measurement





# STATUS OF THE PAPER

• Answers received from referees

• Mainly minor comments and additional explanation required

• Answers prepared, article's text figures re-modified

• We'll submit the new version before the end of the week

6 — G. Galati, A. Alexandro, B. Alpat, G. Ambrosi, S. Argiro, R. Arrese-Diaz, N. Bartosik, G. Battistoni, N. Belcar, E. Bellinzona, S. Bondi, M. G.

**Abstract:** The FOOT (FragmentationOn Target) experiment is an international project dedicated to carry out the fragmentation cross-section measurements relevant for Charged Particle Therapy (CPT), a technique based on the use of charged particle beams for the treatment of deep-seated tumors. The FOOT detector consists of an electronic setup for the identification of  $Z \geq 3$  fragments and of an emulsion spectrometer for  $Z \leq 3$  fragments. The first data taking was performed in 2019 at the GSI facility (Darmstadt, Germany). In this paper, the charge identification of fragments induced by expanding an emulsion detector, embedding a  $C_3H_8$  target, to an Oxygen ion beam of 200 MeV/u is discussed. The charge identification is based on controlled fading of nuclear emulsions in order to extend their dynamic range in the ionization response.

**Keywords:** Particle detector, nuclear emulsion, fragmentation.

**PACS:** 29.40.Rg, 42.62.Bc

## 1 Introduction

Charged Particle Therapy (CPT) is an established therapy for cancer treatment. The advantages of CPT are due to the energy release occurring mainly at the end

of the particle path, in the Bragg peak region, and to the enhanced biological effectiveness of hadron beams, measured in terms of Relative Biological Effectiveness (RBE). The RBE value, defined as the ratio of photon to charged particle doses producing the same biological effect, is assumed to be an average value of 1.1 for proton beams [2]. This value is affected by both physical (i.e. particle type, dose, Linear Energy Transfer) and biological parameters (i.e. tissue type, cell cycle phase, oxygenation level) [2], and many recent studies highly support a comprehensive analysis to reduce uncertainties on the RBE value for the clinical practice [3, 20, 22]. Regarding physical parameters, target fragmentation plays a key role in low energy secondary fragments contribute to increase the dose deposition in normal tissues along the entrance channel and in the region surrounding the target. Hence, the measurement of the proton RBE value due to secondary fragmentation is an important topic [22]. The complexity of dedicated experiments makes this milestone challenging, and in fact very few and limited experiments data are available in literature regarding target fragmentation, and none of them fully describes secondary fragments induced by a proton beam. The fragmentation of carbon ions (400 MeV/u) in a polycarbonate target was studied in 2011 to determine the charge-changing cross-sections by exploiting the nuclear emulsion technique [1].

In this framework, the FOOT (FragmentationOn Target) experiment [1, 16] has been proposed to measure target fragmentation induced by a proton beam in the human tissue in the energy range relevant for therapeutic applications (100 – 500 MeV for protons and 200–400 MeV/u for carbon ions). As fragments generated by a proton beam have low microsecond range, an inverse kinematic approach has been adopted in which a primary beam (carbon or Oxygen) impinge on targets made of carbon and hydrogen-nitrogen-carbon materials ( $C_3H_8$ ). Therefore, the cross-section on hydrogen is derived from their linear combination.

FOOT is based by two complementary setups: a magnetic spectrometer, employing a polar angle acceptance up to about  $10^\circ$  with respect to the beam axis, for fragments  $Z \geq 3$ , and an emulsion spectrometer, to measure light fragments ( $Z \leq 3$ ) up to  $90^\circ$  with respect to the beam axis.

In this paper, the charge identification performance of the secondary fragments generated by the interaction of  $^{16}O$  (200 MeV/u) primary beam on a  $C_3H_8$  target, dispersed in the plastic emulsion, is presented.

The method for the charge identification is based on an established technique already performed in previous

DE GRUYTER: Galati, A. Alexandro, B. Alpat, G. Ambrosi, S. Argiro, R. Arrese-Diaz, N. Bartosik, G. Battistoni, N. Belcar, E. Bellinzona, S. Bondi, M. G.

studies [10, 18, 19], consisting of a controlled fading of nuclear emulsions by means of different thermal treatments, in order to extend the emulsion response to a broader range and make them sensitive to particles with different ionization power and charge.

## 2 Experimental setup and track reconstruction

In April 2019, an emulsion spectrometer was exposed to 200 MeV/u  $^{16}O$  ion beam at the GSI facility in Darmstadt (Germany). The spectrometer acts both as target and tracking device. The target, made of  $C_3H_8$  layers, was embedded in the detector structure. The exposure setup also included a counter and a beam monitor in order to measure the integrated particle density and their spatial distribution. The experimental approach is shown in Fig. 1.



Fig. 1. Experimental setup of the emulsion spectrometer using the 2019 data taking at GSI facility.

and keep memory their trajectory [16], a sequence of AgBr crystals is embedded along its trajectory, producing a latent image. After a chemical development process, the latent images turn into a sequence of dark silver grains which can be seen with an optical microscope [2]. The detection of these grains depends on the ionization of the particle.

Nuclear emulsion films used in the 2019 FOOT measurements were produced by the Nagoya University (Japan) and Slavich Company (Russia) [75] and 25%, respectively. Their sensitivity corresponds to 30 grains over a track length of 100  $\mu m$  for a Minimum Ionizing Particle (MIP).

From the moment they are produced and until their chemical development, nuclear emulsion films are sensitive to charged particles. In particular, during their lifetime they integrate all particle tracks from cosmic rays and environmental radioactivity. To avoid an unwanted background, before the detector assembly, films were transported in a random order, so that cosmic rays accumulated during that period have a different alignment and cannot be reconstructed or spurious tracks. Nevertheless, they can still contribute to the background in case of random association of two or more aligned base-tracks.

## 2.2 Emulsion spectrometer exposure

The emulsion spectrometer was installed in the core A of the GSI facility. The incident beam flux was monitored by a start counter, made of a thin plastic scintillator and by the beam monitor, consisting of a drift chamber that provides the beam spatial distribution.

The integrated field in emulsion films was set at about 1000 pC/mm<sup>2</sup>, a trade-off between the need to avoid the pile-up of interactions in emulsion and the requirement for large statistics. The corresponding number of triggered events in the start counter was 18375.

The primary beam had a Gaussian shape ( $\sigma = 1$  mm signal), low energy, and was used to scan a square area of 2.4 cm side (in a grid of  $25 \times 25$  points), starting from the center and following a spiral square shape with 1 mm pitch.

## 2.1 Nuclear Emulsion Films

Nuclear emulsion films consist of two 70  $\mu m$  thick emulsion layers called top and bottom layers, deposited on both sides of a 210  $\mu m$  grid support film, resulting in a total thickness of 300  $\mu m$ . A  $\mu$ spyr emulsion contains a large number of small AgBr crystals, dispersed in the plastic emulsion, which are randomly dispersed in plastic. When a charged particle crosses the emulsion layer, it is sensitive to ionizing particles

1 https://www.eurchem.org

6 — G. Galati, A. Alexandro, B. Alpat, G. Ambrosi, S. Argiro, R. Arrese-Diaz, N. Bartosik, G. Battistoni, N. Belcar, E. Bellinzona, S. Bondi, M. G.

## 2.3 Emulsion spectrometer structure

The emulsion spectrometer structure, shown in Fig. 2, was built according to the Emulsion Cloud Chamber (ECC) technique [17], which consists of nuclear emulsion films alternated with passive material layers. The emulsion spectrometer structure is organized in three main sections: Section I acts as target region and detector determination, Section II for the charge identification and Section III for the momentum measurement and, consequently, isotopic identification of fragments.

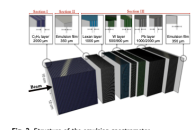


Fig. 2. Structure of the emulsion spectrometer.

## 2.4 Track reconstruction

When a charged particle crosses the emulsion layer, it is sensitive to ionizing particles. After a chemical development process, the latent images turn into a sequence of dark silver grains. Emulsion films were analyzed by flat automated microscope with high tracking efficiency ( $\sim 90\%$ ) and speed (up to 100 cm<sup>2</sup>/hour) [4–6]. The automated scanning system consists of a microscope equipped with a 3D motorized translation stage, a dedicated optical system and a CCD camera.

During the scanning, silver grains produced by the particles are recognized as aligned chains of dark pixels and associated to form the so-called micro-track in the emulsion layer, as shown in Fig. 3. For each film, micro-tracks on the top and bottom layers are then connected across the plastic base to form a base-track, with an accuracy of about 0.3  $\mu m$  in position and 1.2  $\mu m$  in angle. A sequence of base-tracks in different emulsion films allows to reconstruct the particle trajectory inside the detector, called track [8].

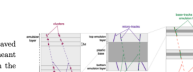


Fig. 3. Schematic drawing of a micro-track reconstruction in different emulsion films, graded at equally spaced depth from the entrance layer (left) to the exit layer (right). The track is formed by the connection of base-tracks in different emulsion films.

The sum of all points corresponding to the same track is proportional to the specific ionization of the incident particle.

## 3 Charge identification

In nuclear emulsions, the grain density along particle tracks is proportional to the particle energy loss over a certain distance range. For highly ionizing particles, such as the ion beam considered here and induced fragments, a saturation effect occurs due to the limited range of the grain density, thus preventing the charge measurement.

Each of these variables was fitted with three gaussian functions, as shown in Fig. 11. To this gaussian fit the particle population with increasing  $Z$  was associated: violet for  $Z = 2$  fragments, pink for  $Z = 3$  and green for  $Z \geq 4$  ones. The fit model has been inferred by the study of a high-purity sample requiring tracks crossing at least 7 cells ( $N_{TR} \geq 7$ ). With the cut-based analysis, a fraction of  $Z = 2$  fragments was already identified. Therefore, in the complementary sample, which survived after the more aggressive thermal treatment applied on  $R2$  and  $R3$ , the component of  $Z = 2$  fragments with higher ionization (lower energy) is expected. For this reason, the  $Z = 2$  gaussian will be partially erased. The threshold value depends on the particle energy and on the statistical fluctuations in the number of ionized grains along the track. These effects produced a smearing in the threshold which is not expected to be large. Therefore, the fit is not taking into account the  $VP_{P25}$  values, where the behavior is not gaussian. Another requirement is that the height of  $Z = 2$  gaussian peak must be higher than that of the  $Z = 3$  gaussian, which in turn has to be higher than or equal to the height of the  $Z = 4$  gaussian, since the number of fragments is expected to decrease as  $Z$  increases.

Excluding cosmic rays from the sample, with the cut-based analysis the charge has been measured for 74% of fragments. A summary of the charge measured is reported in table 2, compared with the distribution of other fragments whose charge was measured with the cut-based analysis.

Each of these variables was fitted with three gaussian functions, as shown in Fig. 11. To this gaussian fit the particle population with increasing  $Z$  was associated: violet for  $Z = 2$  fragments, pink for  $Z = 3$  and green for  $Z \geq 4$  ones. The fit model has been inferred by the study of a high-purity sample requiring tracks crossing at least 7 cells ( $N_{TR} \geq 7$ ). With the cut-based analysis, a fraction of  $Z = 2$  fragments was already identified. Therefore, in the complementary sample, which survived after the more aggressive thermal treatment applied on  $R2$  and  $R3$ , the component of  $Z = 2$  fragments with higher ionization (lower energy) is expected. For this reason, the  $Z = 2$  gaussian will be partially erased. The threshold value depends on the particle energy and on the statistical fluctuations in the number of ionized grains along the track. These effects produced a smearing in the threshold which is not expected to be large. Therefore, the fit is not taking into account the  $VP_{P25}$  values, where the behavior is not gaussian. Another requirement is that the height of  $Z = 2$  gaussian peak must be higher than that of the  $Z = 3$  gaussian, which in turn has to be higher than or equal to the height of the  $Z = 4$  gaussian, since the number of fragments is expected to decrease as  $Z$  increases.

Excluding cosmic rays from the sample, with the cut-based analysis the charge has been measured for 74% of fragments. A summary of the charge measured is reported in table 2, compared with the distribution of other fragments whose charge was measured with the cut-based analysis.

Each of these variables was fitted with three gaussian functions, as shown in Fig. 11. To this gaussian fit the particle population with increasing  $Z$  was associated: violet for  $Z = 2$  fragments, pink for  $Z = 3$  and green for  $Z \geq 4$  ones. The fit model has been inferred by the study of a high-purity sample requiring tracks crossing at least 7 cells ( $N_{TR} \geq 7$ ). With the cut-based analysis, a fraction of  $Z = 2$  fragments was already identified. Therefore, in the complementary sample, which survived after the more aggressive thermal treatment applied on  $R2$  and  $R3$ , the component of  $Z = 2$  fragments with higher ionization (lower energy) is expected. For this reason, the  $Z = 2$  gaussian will be partially erased. The threshold value depends on the particle energy and on the statistical fluctuations in the number of ionized grains along the track. These effects produced a smearing in the threshold which is not expected to be large. Therefore, the fit is not taking into account the  $VP_{P25}$  values, where the behavior is not gaussian. Another requirement is that the height of  $Z = 2$  gaussian peak must be higher than that of the  $Z = 3$  gaussian, which in turn has to be higher than or equal to the height of the  $Z = 4$  gaussian, since the number of fragments is expected to decrease as  $Z$  increases.

Excluding cosmic rays from the sample, with the cut-based analysis the charge has been measured for 74% of fragments. A summary of the charge measured is reported in table 2, compared with the distribution of other fragments whose charge was measured with the cut-based analysis.

Each of these variables was fitted with three gaussian functions, as shown in Fig. 11. To this gaussian fit the particle population with increasing  $Z$  was associated: violet for  $Z = 2$  fragments, pink for  $Z = 3$  and green for  $Z \geq 4$  ones. The fit model has been inferred by the study of a high-purity sample requiring tracks crossing at least 7 cells ( $N_{TR} \geq 7$ ). With the cut-based analysis, a fraction of  $Z = 2$  fragments was already identified. Therefore, in the complementary sample, which survived after the more aggressive thermal treatment applied on  $R2$  and  $R3$ , the component of  $Z = 2$  fragments with higher ionization (lower energy) is expected. For this reason, the  $Z = 2$  gaussian will be partially erased. The threshold value depends on the particle energy and on the statistical fluctuations in the number of ionized grains along the track. These effects produced a smearing in the threshold which is not expected to be large. Therefore, the fit is not taking into account the  $VP_{P25}$  values, where the behavior is not gaussian. Another requirement is that the height of  $Z = 2$  gaussian peak must be higher than that of the  $Z = 3$  gaussian, which in turn has to be higher than or equal to the height of the  $Z = 4$  gaussian, since the number of fragments is expected to decrease as  $Z$  increases.

Excluding cosmic rays from the sample, with the cut-based analysis the charge has been measured for 74% of fragments. A summary of the charge measured is reported in table 2, compared with the distribution of other fragments whose charge was measured with the cut-based analysis.

Each of these variables was fitted with three gaussian functions, as shown in Fig. 11. To this gaussian fit the particle population with increasing  $Z$  was associated: violet for  $Z = 2$  fragments, pink for  $Z = 3$  and green for  $Z \geq 4$  ones. The fit model has been inferred by the study of a high-purity sample requiring tracks crossing at least 7 cells ( $N_{TR} \geq 7$ ). With the cut-based analysis, a fraction of  $Z = 2$  fragments was already identified. Therefore, in the complementary sample, which survived after the more aggressive thermal treatment applied on  $R2$  and  $R3$ , the component of  $Z = 2$  fragments with higher ionization (lower energy) is expected. For this reason, the  $Z = 2$  gaussian will be partially erased. The threshold value depends on the particle energy and on the statistical fluctuations in the number of ionized grains along the track. These effects produced a smearing in the threshold which is not expected to be large. Therefore, the fit is not taking into account the  $VP_{P25}$  values, where the behavior is not gaussian. Another requirement is that the height of  $Z = 2$  gaussian peak must be higher than that of the  $Z = 3$  gaussian, which in turn has to be higher than or equal to the height of the  $Z = 4$  gaussian, since the number of fragments is expected to decrease as  $Z$  increases.

Excluding cosmic rays from the sample, with the cut-based analysis the charge has been measured for 74% of fragments. A summary of the charge measured is reported in table 2, compared with the distribution of other fragments whose charge was measured with the cut-based analysis.

Each of these variables was fitted with three gaussian functions, as shown in Fig. 11. To this gaussian fit the particle population with increasing  $Z$  was associated: violet for  $Z = 2$  fragments, pink for  $Z = 3$  and green for  $Z \geq 4$  ones. The fit model has been inferred by the study of a high-purity sample requiring tracks crossing at least 7 cells ( $N_{TR} \geq 7$ ). With the cut-based analysis, a fraction of  $Z = 2$  fragments was already identified. Therefore, in the complementary sample, which survived after the more aggressive thermal treatment applied on  $R2$  and  $R3$ , the component of  $Z = 2$  fragments with higher ionization (lower energy) is expected. For this reason, the  $Z = 2$  gaussian will be partially erased. The threshold value depends on the particle energy and on the statistical fluctuations in the number of ionized grains along the track. These effects produced a smearing in the threshold which is not expected to be large. Therefore, the fit is not taking into account the  $VP_{P25}$  values, where the behavior is not gaussian. Another requirement is that the height of  $Z = 2$  gaussian peak must be higher than that of the  $Z = 3$  gaussian, which in turn has to be higher than or equal to the height of the  $Z = 4$  gaussian, since the number of fragments is expected to decrease as  $Z$  increases.

Excluding cosmic rays from the sample, with the cut-based analysis the charge has been measured for 74% of fragments. A summary of the charge measured is reported in table 2, compared with the distribution of other fragments whose charge was measured with the cut-based analysis.

Each of these variables was fitted with three gaussian functions, as shown in Fig. 11. To this gaussian fit the particle population with increasing  $Z$  was associated: violet for  $Z = 2$  fragments, pink for  $Z = 3$  and green for  $Z \geq 4$  ones. The fit model has been inferred by the study of a high-purity sample requiring tracks crossing at least 7 cells ( $N_{TR} \geq 7$ ). With the cut-based analysis, a fraction of  $Z = 2$  fragments was already identified. Therefore, in the complementary sample, which survived after the more aggressive thermal treatment applied on  $R2$  and  $R3$ , the component of  $Z = 2$  fragments with higher ionization (lower energy) is expected. For this reason, the  $Z = 2$  gaussian will be partially erased. The threshold value depends on the particle energy and on the statistical fluctuations in the number of ionized grains along the track. These effects produced a smearing in the threshold which is not expected to be large. Therefore, the fit is not taking into account the  $VP_{P25}$  values, where the behavior is not gaussian. Another requirement is that the height of  $Z = 2$  gaussian peak must be higher than that of the  $Z = 3$  gaussian, which in turn has to be higher than or equal to the height of the  $Z = 4$  gaussian, since the number of fragments is expected to decrease as  $Z$  increases.

Excluding cosmic rays from the sample, with the cut-based analysis the charge has been measured for 74% of fragments. A summary of the charge measured is reported in table 2, compared with the distribution of other fragments whose charge was measured with the cut-based analysis.

Each of these variables was fitted with three gaussian functions, as shown in Fig. 11. To this gaussian fit the particle population with increasing  $Z$  was associated: violet for  $Z = 2$  fragments, pink for  $Z = 3$  and green for  $Z \geq 4$  ones. The fit model has been inferred by the study of a high-purity sample requiring tracks crossing at least 7 cells ( $N_{TR} \geq 7$ ). With the cut-based analysis, a fraction of  $Z = 2$  fragments was already identified. Therefore, in the complementary sample, which survived after the more aggressive thermal treatment applied on  $R2$  and  $R3$ , the component of  $Z = 2$  fragments with higher ionization (lower energy) is expected. For this reason, the  $Z = 2$  gaussian will be partially erased. The threshold value depends on the particle energy and on the statistical fluctuations in the number of ionized grains along the track. These effects produced a smearing in the threshold which is not expected to be large. Therefore, the fit is not taking into account the  $VP_{P25}$  values, where the behavior is not gaussian. Another requirement is that the height of  $Z = 2$  gaussian peak must be higher than that of the  $Z = 3$  gaussian, which in turn has to be higher than or equal to the height of the  $Z = 4$  gaussian, since the number of fragments is expected to decrease as  $Z$  increases.

Excluding cosmic rays from the sample, with the cut-based analysis the charge has been measured for 74% of fragments. A summary of the charge measured is reported in table 2, compared with the distribution of other fragments whose charge was measured with the cut-based analysis.

Each of these variables was fitted with three gaussian functions, as shown in Fig. 11. To this gaussian fit the particle population with increasing  $Z$  was associated: violet for  $Z = 2$  fragments, pink for  $Z = 3$  and green for  $Z \geq 4$  ones. The fit model has been inferred by the study of a high-purity sample requiring tracks crossing at least 7 cells ( $N_{TR} \geq 7$ ). With the cut-based analysis, a fraction of  $Z = 2$  fragments was already identified. Therefore, in the complementary sample, which survived after the more aggressive thermal treatment applied on  $R2$  and  $R3$ , the component of  $Z = 2$  fragments with higher ionization (lower energy) is expected. For this reason, the  $Z = 2$  gaussian will be partially erased. The threshold value depends on the particle energy and on the statistical fluctuations in the number of ionized grains along the track. These effects produced a smearing in the threshold which is not expected to be large. Therefore, the fit is not taking into account the  $VP_{P25}$  values, where the behavior is not gaussian. Another requirement is that the height of  $Z = 2$  gaussian peak must be higher than that of the  $Z = 3$  gaussian, which in turn has to be higher than or equal to the height of the  $Z = 4$  gaussian, since the number of fragments is expected to decrease as  $Z$  increases.

Excluding cosmic rays from the sample, with the cut-based analysis the charge has been measured for 74% of fragments. A summary of the charge measured is reported in table 2, compared with the distribution of other fragments whose charge was measured with the cut-based analysis.

Each of these variables was fitted with three gaussian functions, as shown in Fig. 11. To this gaussian fit the particle population with increasing  $Z$  was associated: violet for  $Z = 2$  fragments, pink for  $Z = 3$  and green for  $Z \geq 4$  ones. The fit model has been inferred by the study of a high-purity sample requiring tracks crossing at least 7 cells ( $N_{TR} \geq 7$ ). With the cut-based analysis, a fraction of  $Z = 2$  fragments was already identified. Therefore, in the complementary sample, which survived after the more aggressive thermal treatment applied on  $R2$  and  $R3$ , the component of  $Z = 2$  fragments with higher ionization (lower energy) is expected. For this reason, the  $Z = 2$  gaussian will be partially erased. The threshold value depends on the particle energy and on the statistical fluctuations in the number of ionized grains along the track. These effects produced a smearing in the threshold which is not expected to be large. Therefore, the fit is not taking into account the  $VP_{P25}$  values, where the behavior is not gaussian. Another requirement is that the height of  $Z = 2$  gaussian peak must be higher than that of the  $Z = 3$  gaussian, which in turn has to be higher than or equal to the height of the  $Z = 4$  gaussian, since the number of fragments is expected to decrease as  $Z$  increases.

Excluding cosmic rays from the sample, with the cut-based analysis the charge has been measured for 74% of fragments. A summary of the charge measured is reported in table 2, compared with the distribution of other fragments whose charge was measured with the cut-based analysis.

Each of these variables was fitted with three gaussian functions, as shown in Fig. 11. To this gaussian fit the particle population with increasing  $Z$  was associated: violet for  $Z = 2$  fragments, pink for  $Z = 3$  and green for  $Z \geq 4$  ones. The fit model has been inferred by the study of a high-purity sample requiring tracks crossing at least 7 cells ( $N_{TR} \geq 7$ ). With the cut-based analysis, a fraction of  $Z = 2$  fragments was already identified. Therefore, in the complementary sample, which survived after the more aggressive thermal treatment applied on  $R2$  and  $R3$ , the component of  $Z = 2$  fragments with higher ionization (lower energy) is expected. For this reason, the  $Z = 2$  gaussian will be partially erased. The threshold value depends on the particle energy and on the statistical fluctuations in the number of ionized grains along the track. These effects produced a smearing in the threshold which is not expected to be large. Therefore, the fit is not taking into account the  $VP_{P25}$  values, where the behavior is not gaussian. Another requirement is that the height of  $Z = 2$  gaussian peak must be higher than that of the  $Z = 3$  gaussian, which in turn has to be higher than or equal to the height of the  $Z = 4$  gaussian, since the number of fragments is expected to decrease as  $Z$  increases.

Excluding cosmic rays from the sample, with the cut-based analysis the charge has been measured for 74% of fragments. A summary of the charge measured is reported in table 2, compared with the distribution of other fragments whose charge was measured with the cut-based analysis.

Each of these variables was fitted with three gaussian functions, as shown in Fig. 11. To this gaussian fit the particle population with increasing  $Z$  was associated: violet for  $Z = 2$  fragments, pink for  $Z = 3$  and green for  $Z \geq 4$  ones. The fit model has been inferred by the study of a high-purity sample requiring tracks crossing at least 7 cells ( $N_{TR} \geq 7$ ). With the cut-based analysis, a fraction of  $Z = 2$  fragments was already identified. Therefore, in the complementary sample, which survived after the more aggressive thermal treatment applied on  $R2$  and  $R3$ , the component of  $Z = 2$  fragments with higher ionization (lower energy) is expected. For this reason, the  $Z = 2$  gaussian will be partially erased. The threshold value depends on the particle energy and on the statistical fluctuations in the number of ionized grains along the track. These effects produced a smearing in the threshold which is not expected to be large. Therefore, the fit is not taking into account the  $VP_{P25}$  values, where the behavior is not gaussian. Another requirement is that the height of  $Z = 2$  gaussian peak must be higher than that of the  $Z = 3$  gaussian, which in turn has to be higher than or equal to the height of the  $Z = 4$  gaussian, since the number of fragments is expected to decrease as  $Z$  increases.

Excluding cosmic rays from the sample, with the cut-based analysis the charge has been measured for 74% of fragments. A summary of the charge measured is reported in table 2, compared with the distribution of other fragments whose charge was measured with the cut-based analysis.

Each of these variables was fitted with three gaussian functions, as shown in Fig. 11. To this gaussian fit the particle population with increasing  $Z$  was associated: violet for  $Z = 2$  fragments, pink for  $Z = 3$  and green for  $Z \geq 4$  ones. The fit model has been inferred by the study of a high-purity sample requiring tracks crossing at least 7 cells ( $N_{TR} \geq 7$ ). With the cut-based analysis, a fraction of  $Z = 2$  fragments was already identified. Therefore, in the complementary sample, which survived after the more aggressive thermal treatment applied on  $R2$  and  $R3$ , the component of  $Z = 2$  fragments with higher ionization (lower energy) is expected. For this reason, the  $Z = 2$  gaussian will be partially erased. The threshold value depends on the particle energy and on the statistical fluctuations in the number of ionized grains along the track. These effects produced a smearing in the threshold which is not expected to be large. Therefore, the fit is not taking into account the  $VP_{P25}$  values, where the behavior is not gaussian. Another requirement is that the height of  $Z = 2$  gaussian peak must be higher than that of the  $Z = 3$  gaussian, which in turn has to be higher than or equal to the height of the  $Z = 4$  gaussian, since the number of fragments is expected to decrease as  $Z$  increases.

Excluding cosmic rays from the sample, with the cut-based analysis the charge has been measured for 74% of fragments. A summary of the charge measured is reported in table 2, compared with the distribution of other fragments whose charge was measured with the cut-based analysis.

Each of these variables was fitted with three gaussian functions, as shown in Fig. 11. To this gaussian fit the particle population with increasing  $Z$  was associated: violet for  $Z = 2$  fragments, pink for  $Z = 3$  and green for  $Z \geq 4$  ones. The fit model has been inferred by the study of a high-purity sample requiring tracks crossing at least 7 cells ( $N_{TR} \geq 7$ ). With the cut-based analysis, a fraction of  $Z = 2$  fragments was already identified. Therefore, in the complementary sample, which survived after the more aggressive thermal treatment applied on  $R2$  and  $R3$ , the component of  $Z = 2$  fragments with higher ionization (lower energy) is expected. For this reason, the  $Z = 2$  gaussian will be partially erased. The threshold value depends on the particle energy and on the statistical fluctuations in the number of ionized grains along the track. These effects produced a smearing in the threshold which is not expected to be large. Therefore, the fit is not taking into account the  $VP_{P25}$  values, where the behavior is not gaussian. Another requirement is that the height of  $Z = 2$  gaussian peak must be higher than that of the  $Z = 3$  gaussian, which in turn has to be higher than or equal to the height of the  $Z = 4$  gaussian, since the number of fragments is expected to decrease as  $Z$  increases.

Excluding cosmic rays from the sample, with the cut-based analysis the charge has been measured for 74% of fragments. A summary of the charge measured is reported in table 2, compared with the distribution of other fragments whose charge was measured with the cut-based analysis.

Each of these variables was fitted with three gaussian functions, as shown in Fig. 11. To this gaussian fit the particle population with increasing  $Z$  was associated: violet for  $Z = 2$  fragments, pink for  $Z = 3$  and green for  $Z \geq 4$  ones. The fit model has been inferred by the study of a high-purity sample requiring tracks crossing at least 7 cells ( $N_{TR} \geq 7$ ). With the cut-based analysis, a fraction of  $Z = 2$  fragments was already identified. Therefore, in the complementary sample, which survived after the more aggressive thermal treatment applied on  $R2$  and  $R3$ , the component of  $Z = 2$  fragments with higher ionization (lower energy) is expected. For this reason, the  $Z = 2$  gaussian will be partially erased. The threshold value depends on the particle energy and on the statistical fluctuations in the number of ionized grains along the track. These effects produced a smearing in the threshold which is not expected to be large. Therefore, the fit is not taking into account the  $VP_{P25}$  values, where the behavior is not gaussian. Another requirement is that the height of  $Z = 2$  gaussian peak must be higher than that of the  $Z = 3$  gaussian, which in turn has to be higher than or equal to the height of the  $Z = 4$  gaussian, since the number of fragments is expected to decrease as  $Z$  increases.

Excluding cosmic rays from the sample, with the cut-based analysis the charge has been measured for 74% of fragments. A summary of the charge measured is reported in table 2, compared with the distribution of other fragments whose charge was measured with the cut-based analysis.

Each of these variables was fitted with three gaussian functions, as shown in Fig. 11. To this gaussian fit the particle population with increasing  $Z$  was associated: violet for  $Z = 2$  fragments, pink for  $Z = 3$  and green for  $Z \geq 4$  ones. The fit model has been inferred by the study of a high-purity sample requiring tracks crossing at least 7 cells ( $N_{TR} \geq 7$ ). With the cut-based analysis, a fraction of  $Z = 2$  fragments was already identified. Therefore, in the complementary sample, which survived after the more aggressive thermal treatment applied on  $R2$  and  $R3$ , the component of  $Z = 2$  fragments with higher ionization (lower energy) is expected. For this reason, the  $Z = 2$  gaussian will be partially erased. The threshold value depends on the particle energy and on the statistical fluctuations in the number of ionized grains along the track. These effects produced a smearing in the threshold which is not expected to be large. Therefore, the fit is not taking into account the  $VP_{P25}$  values, where the behavior is not gaussian. Another requirement is that the height of  $Z = 2$  gaussian peak must be higher than that of the  $Z = 3$  gaussian, which in turn has to be higher than or equal to the height of the  $Z = 4$  gaussian, since the number of fragments is expected to decrease as  $Z$  increases.

Excluding cosmic rays from the sample, with the cut-based analysis the charge has been measured for 74% of fragments. A summary of the charge measured is reported in table 2, compared with the distribution of other fragments whose charge was measured with the cut-based analysis.

Each of these variables was fitted with three gaussian functions, as shown in Fig. 11. To this gaussian fit the particle population with increasing  $Z$  was associated: violet for  $Z = 2$  fragments, pink for  $Z = 3$  and green for  $Z \geq 4$  ones. The fit model has been inferred by the study of a high-purity sample requiring tracks crossing at least 7 cells ( $N_{TR} \geq 7$ ). With the cut-based analysis, a fraction of  $Z = 2$  fragments was already identified. Therefore, in the complementary sample, which survived after the more aggressive thermal treatment applied on  $R2$  and  $R3$ , the component of  $Z = 2$  fragments with higher ionization (lower energy) is expected. For this reason, the  $Z = 2$  gaussian will be partially erased. The threshold value depends on the particle energy and on the statistical fluctuations in the number of ionized grains along the track. These effects produced a smearing in the threshold which is not expected to be large. Therefore, the fit is not taking into account the  $VP_{P25}$  values, where the behavior is not gaussian. Another requirement is that the height of  $Z = 2$  gaussian peak must be higher than that of the  $Z = 3$  gaussian, which in turn has to be higher than or equal to the height of the  $Z = 4$  gaussian, since the number of fragments is expected to decrease as  $Z$  increases.

Excluding cosmic rays from the sample, with the cut-based analysis the charge has been measured for 74% of fragments. A summary of the charge measured is reported in table 2, compared with the distribution of other fragments whose charge was measured with the cut-based analysis.

Each of these variables was fitted with three gaussian functions, as shown in Fig. 11. To this gaussian fit the particle population with increasing  $Z$  was associated: violet for  $Z = 2$  fragments, pink for  $Z = 3$  and green for  $Z \geq 4$  ones. The fit model has been inferred by the study of a high-purity sample requiring tracks crossing at least 7 cells ( $N_{TR} \geq 7$ ). With the cut-based analysis, a fraction of  $Z = 2$  fragments was already identified. Therefore, in the complementary sample, which

# Paper on OPEN PHYSICS

Reviewer #1: The text in figure 10 is very small and difficult to read. Please make this figure bigger so the text and data points are easier to see.

## Reviewer #2

### Major comments

1) Page 5- Lines 52-59 - left column

The procedure used to extract the percentage of combinatorial background (1.7%) should be detailed.

2) Par. 3.2 and Fig. 7

While the presence of two populations (cosmics and  $Z=1$ ) is evident in Fig. 5, the same is not true for Fig. 7. It is not clear to me how the presence of  $Z=2$  fragments can be inferred by data for the class of events reported in Fig. 7. Moreover, the choose of the position of the boundaries between the "two populations" looks to me completely arbitrary. This also affects the associated systematic uncertainties.

The authors should better agree the results of this paragraph or maybe reconsider their interpretation.

3) Page 8 - Lines 44-47 and 53-57 - left column

Authors should specify why the charge assignment is done taking into account the gaussian height and not the integral. What is the meaning of the sigma in the fits of Fig. 10?

### Minor comments

1) Page 3 - Lines 57-60 - left column

The effects of ionizing radiation on AgBr crystals could be described more clearly.

2) Page 3 - Line 39 - right column

Change "primary beam" with "beam"

3) Page 5 - Lines 38-39 - left column

What are the units of the VRx variable? They should be included in all the plots where this variable appears.

# Paper on OPEN PHYSICS

Reviewer #1: The text in figure 10 is very small and difficult to read. Please make this figure bigger so the text and data points are easier to see.

## Reviewer #2

### Major comments

1) Page 5- Lines 52-59 - left column

The procedure used to extract the percentage of combinatorial background (1.7%) should be detailed.

2) Par. 3.2 and Fig. 7

While the presence of two populations (cosmics and  $Z=1$ ) is evident in Fig. 5, the same is not true for Fig. 7. It is not clear to me how the presence of  $Z=2$  fragments can be inferred by data for the class of events reported in Fig. 7. Moreover, the choose of the position of the boundaries between the "two populations" looks to me completely arbitrary. This also affects the associated systematic uncertainties.

The authors should better agree the results of this paragraph or maybe reconsider their interpretation.

3) Page 8 - Lines 44-47 and 53-57 - left column

Authors should specify why the charge assignment is done taking into account the gaussian height and not the integral. What is the meaning of the sigma in the fits of Fig. 10?

### Minor comments

1) Page 3 - Lines 57-60 - left column

The effects of ionizing radiation on AgBr crystals could be described more clearly.

2) Page 3 - Line 39 - right column

Change "primary beam" with "beam"

3) Page 5 - Lines 38-39 - left column

What are the units of the VRx variable? They should be included in all the plots where this variable appears.

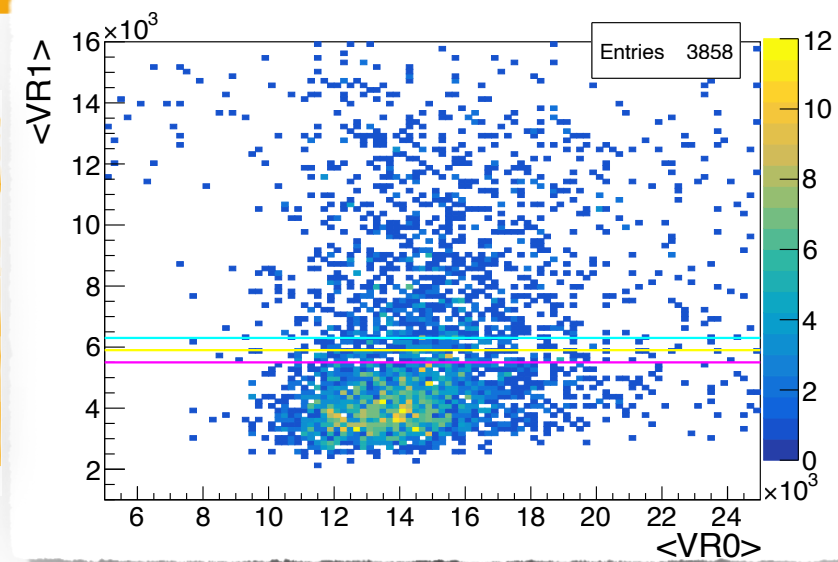


# Paper on OPEN PHYSICS

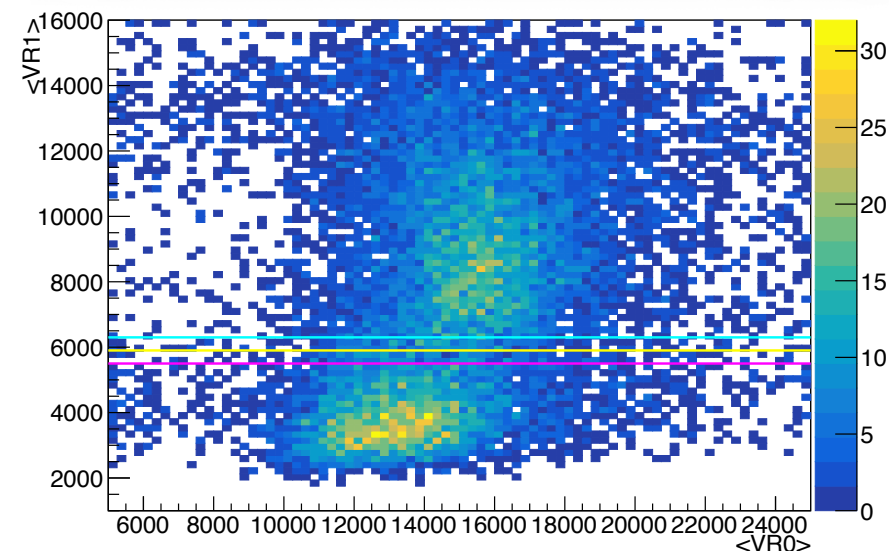
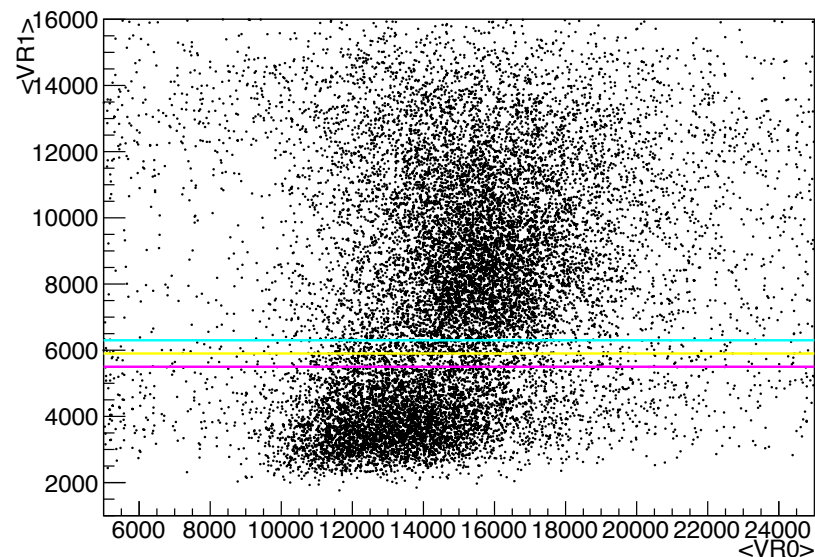
2) Par. 3.2 and Fig. 7

While the presence of two populations (cosmics and  $Z=1$ ) is evident in Fig. 5, the same is not true for Fig. 7. It is not clear to me how the presence of  $Z=2$  fragments can be inferred by data for the class of events reported in Fig. 7. Moreover, the choice of the position of the boundaries between the "two populations" looks to me completely arbitrary. This also affects the associated systematic uncertainties.

The authors should better agree the results of this paragraph or maybe reconsider their interpretation.



- Two populations and their boundaries are confirmed looking at the same plot where no cuts have been applied on NR2 and NR3
- The number of fragments below the cut ( $Z=1$ ) is stable in the two cases
- New plot and related explanation added also in the paper



Distribution of  $\langle VR1 \rangle$  versus  $\langle VR0 \rangle$  for all tracks with  $NR1 > 1$   
No cuts have been applied on NR2 and NR3

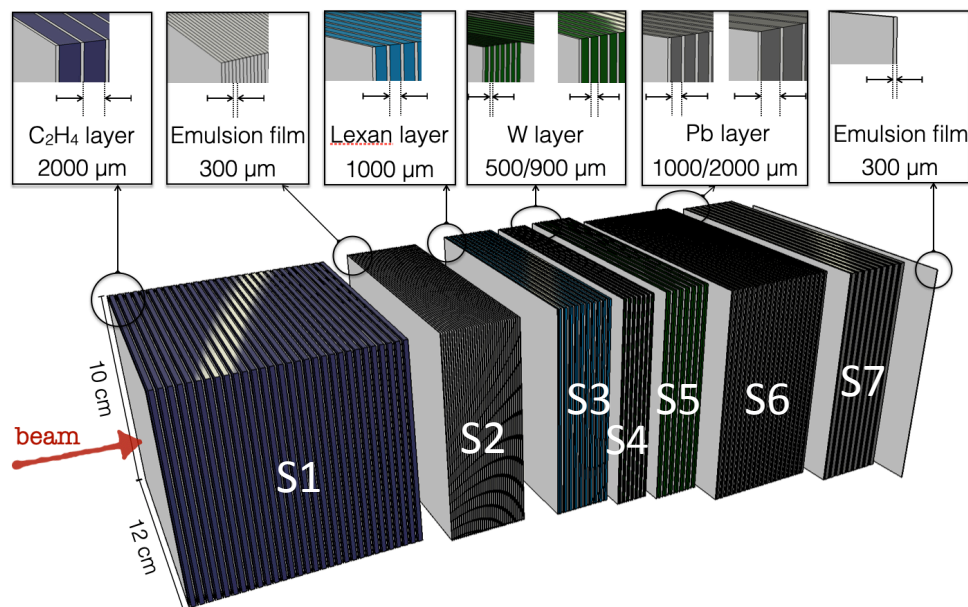


# UPDATES ON THE ANALYSIS



# Scanning Progress

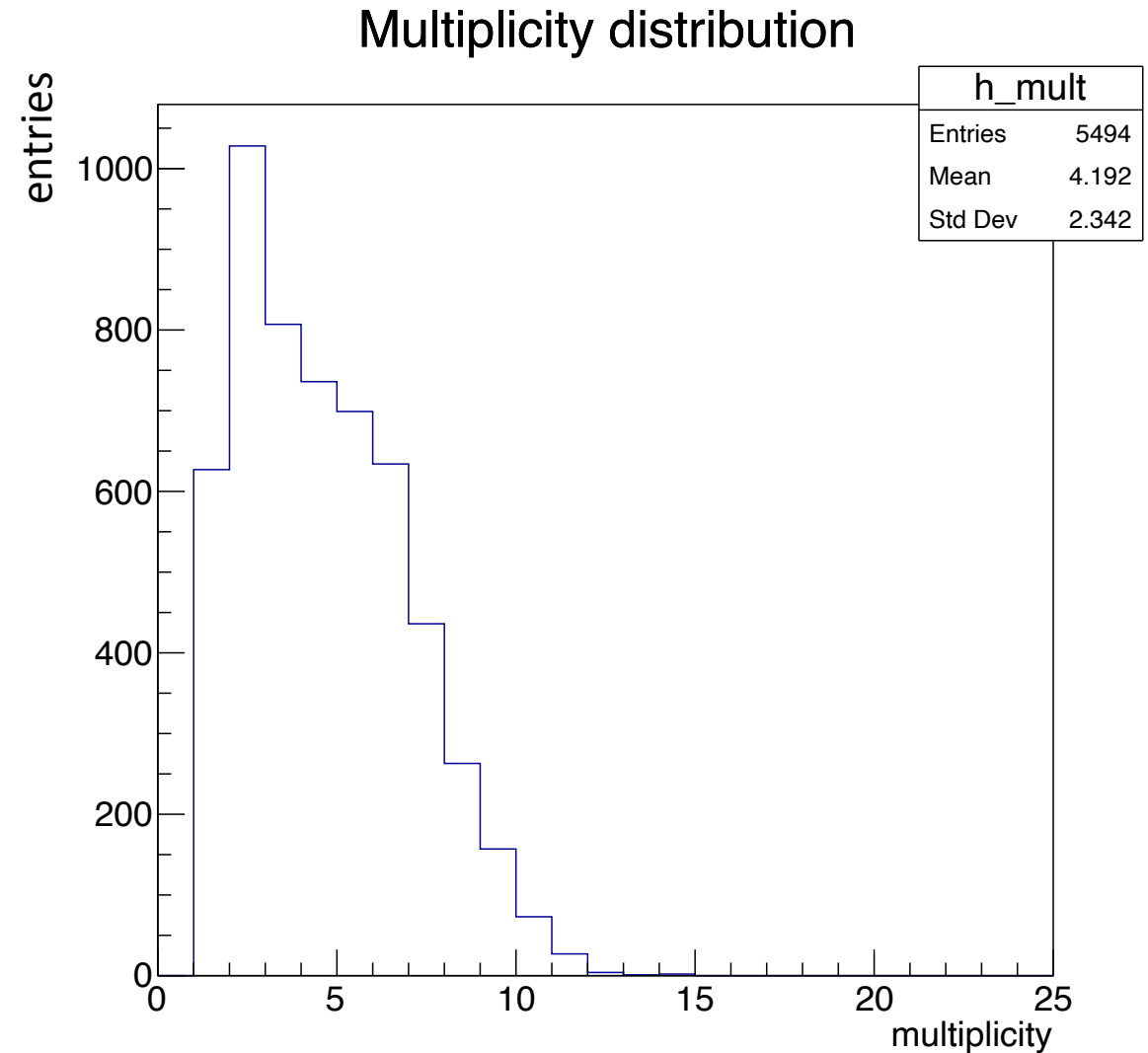
	2019		2020
	Oxygen 200 MeV/n	Oxygen 400 MeV/n	Carbon 700MeV/n
Carbon	GSI1	GSI3	GSI5
Polyethylene	GSI2	GSI4	GSI6



- 2019 (GSI1, GSI2, GSI3, GSI4):
  - scanning: 100%
  - alignment:
    - GSI1: 100%
    - GSI2: 100%
    - GSI3: 47%
    - GSI4: 21%
  - tracking:
    - GSI2: S1+S2 completed, S3 (=S3+S4+S5+S6+S7) started
    - GSI1: S1+S2 quality checks ongoing
- 2020 (GSI5, GSI6):
  - scanning: 328/328 (100%)

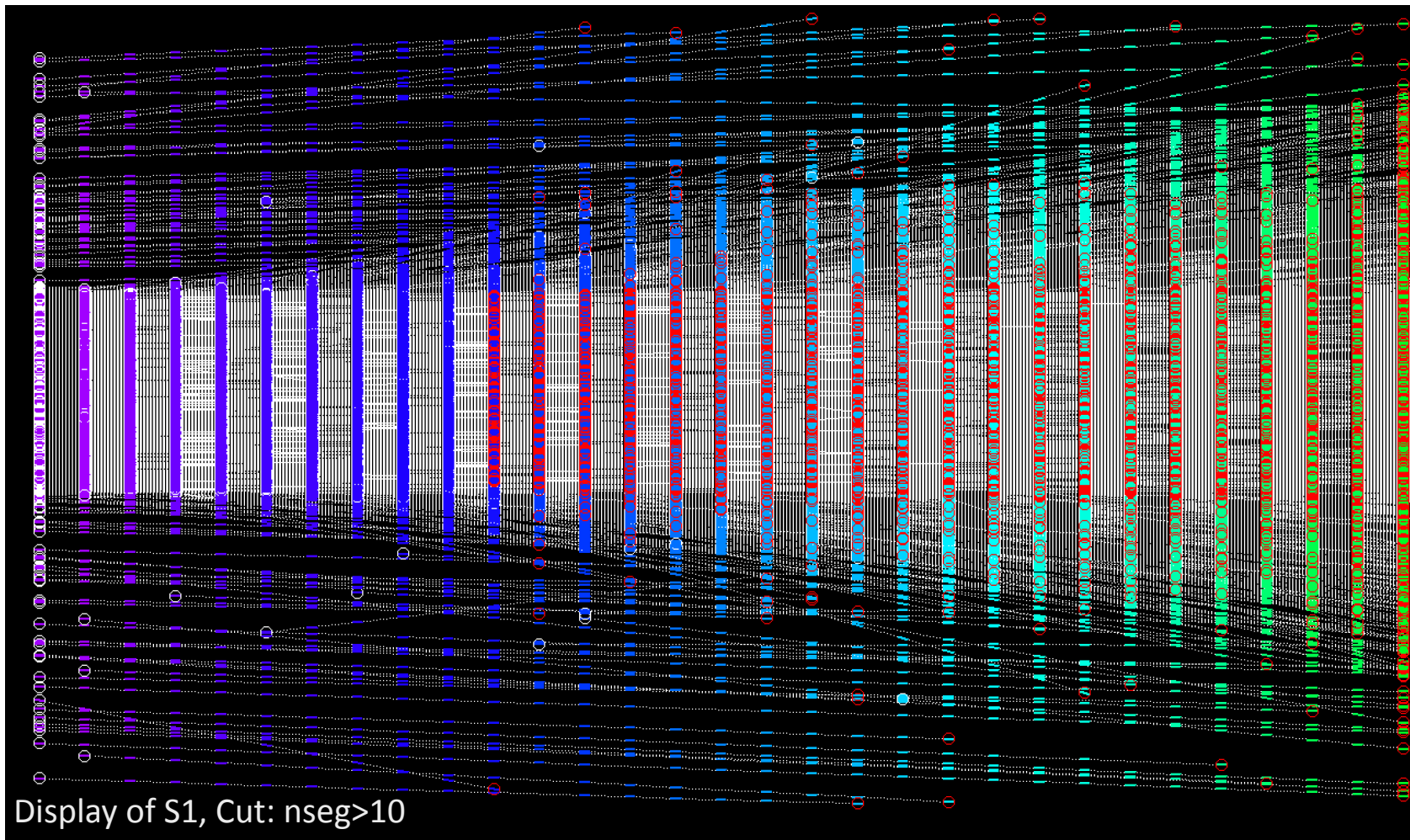
# GSI1: MC Analysis

- New MC simulation with Fluka2020
- 5623 vertices expected in S1
- Mean multiplicity: 4
- 96.2% of tracks contained



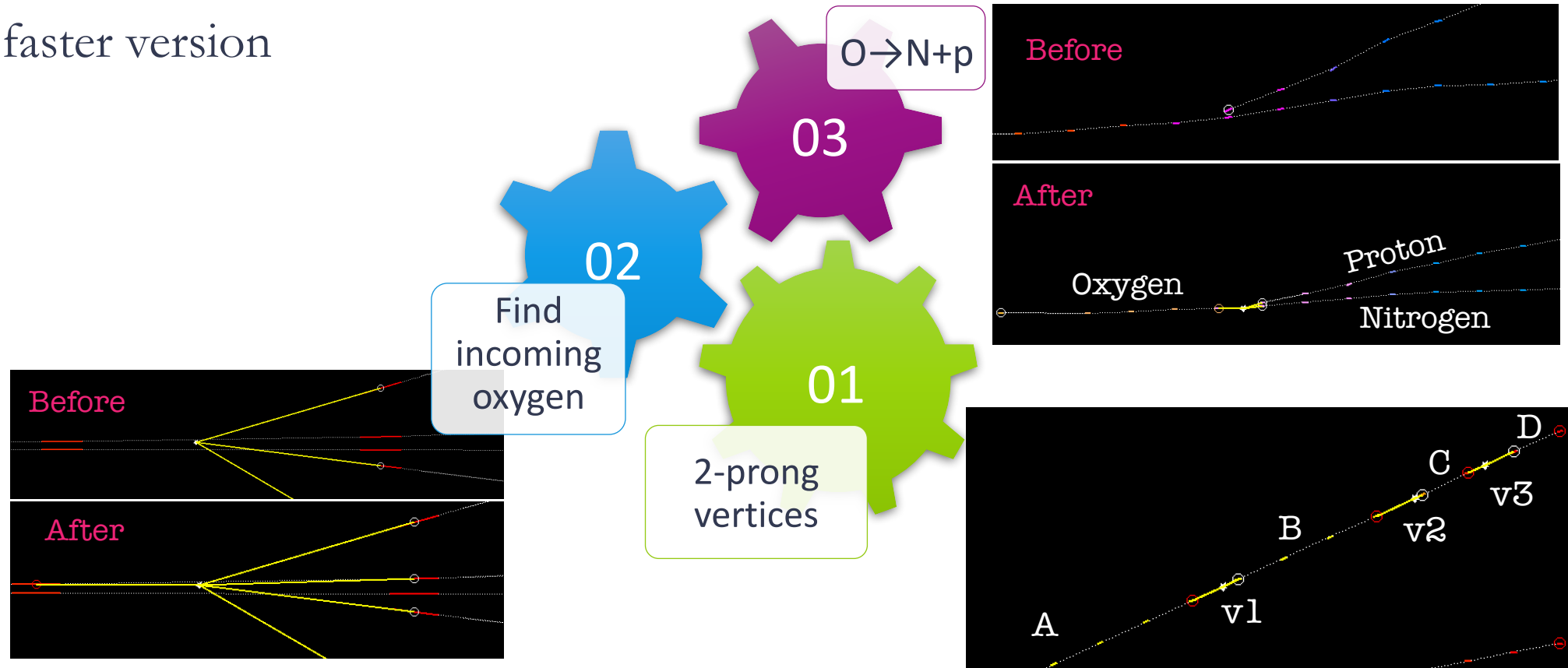
# Tracks reconstruction

- MC exported in data format, with smearing and inefficiencies
- Combinatorial background due to spare base tracks added to MC



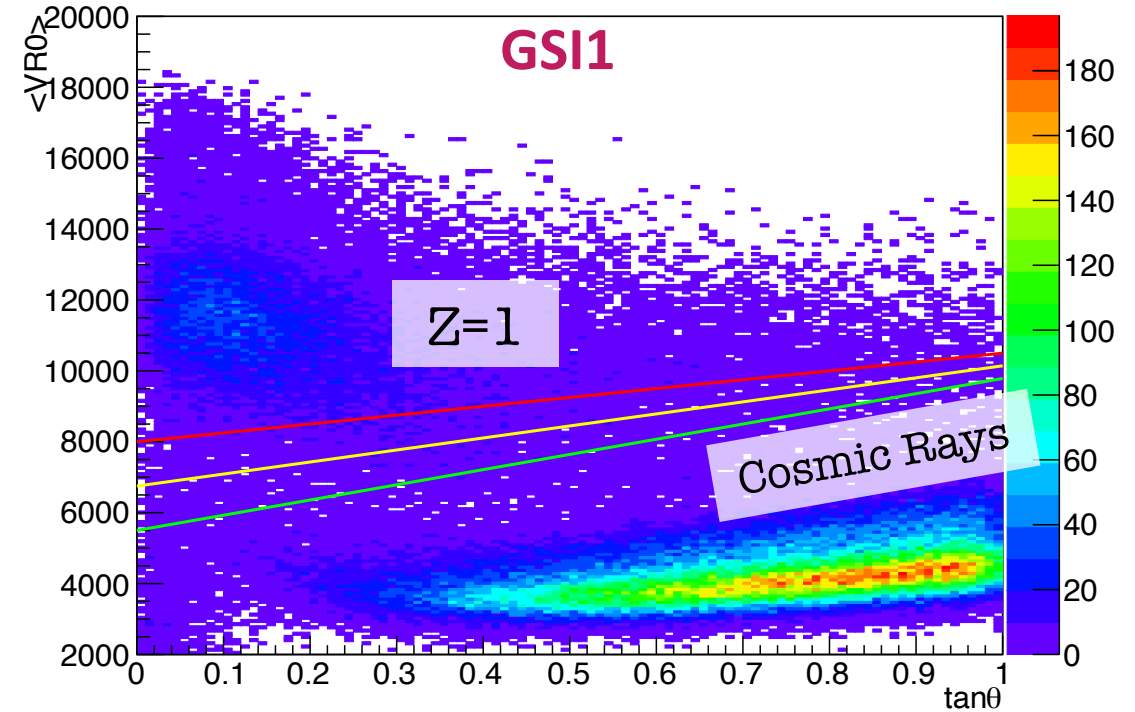
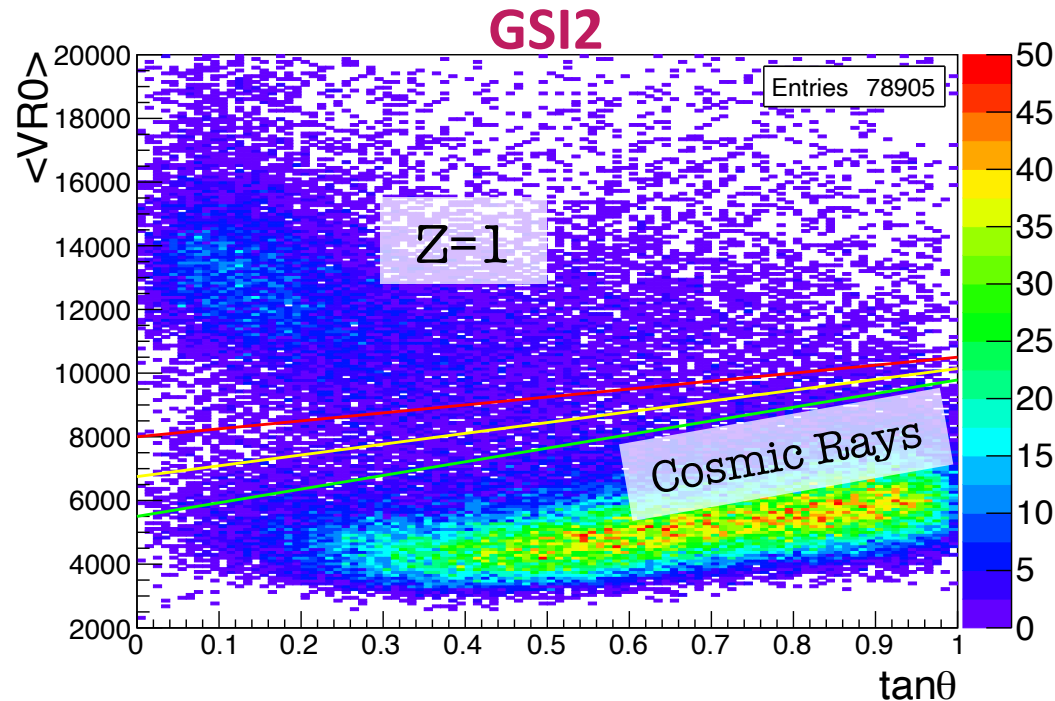
# Vertices Reconstruction (MC)

- 5188 vertices reconstructed with at least 3 tracks
- Vertices quality improvements: ongoing
- Algorithm too slow
- Working on a faster version
- Working on purity of  $O \rightarrow N+p$  topologies

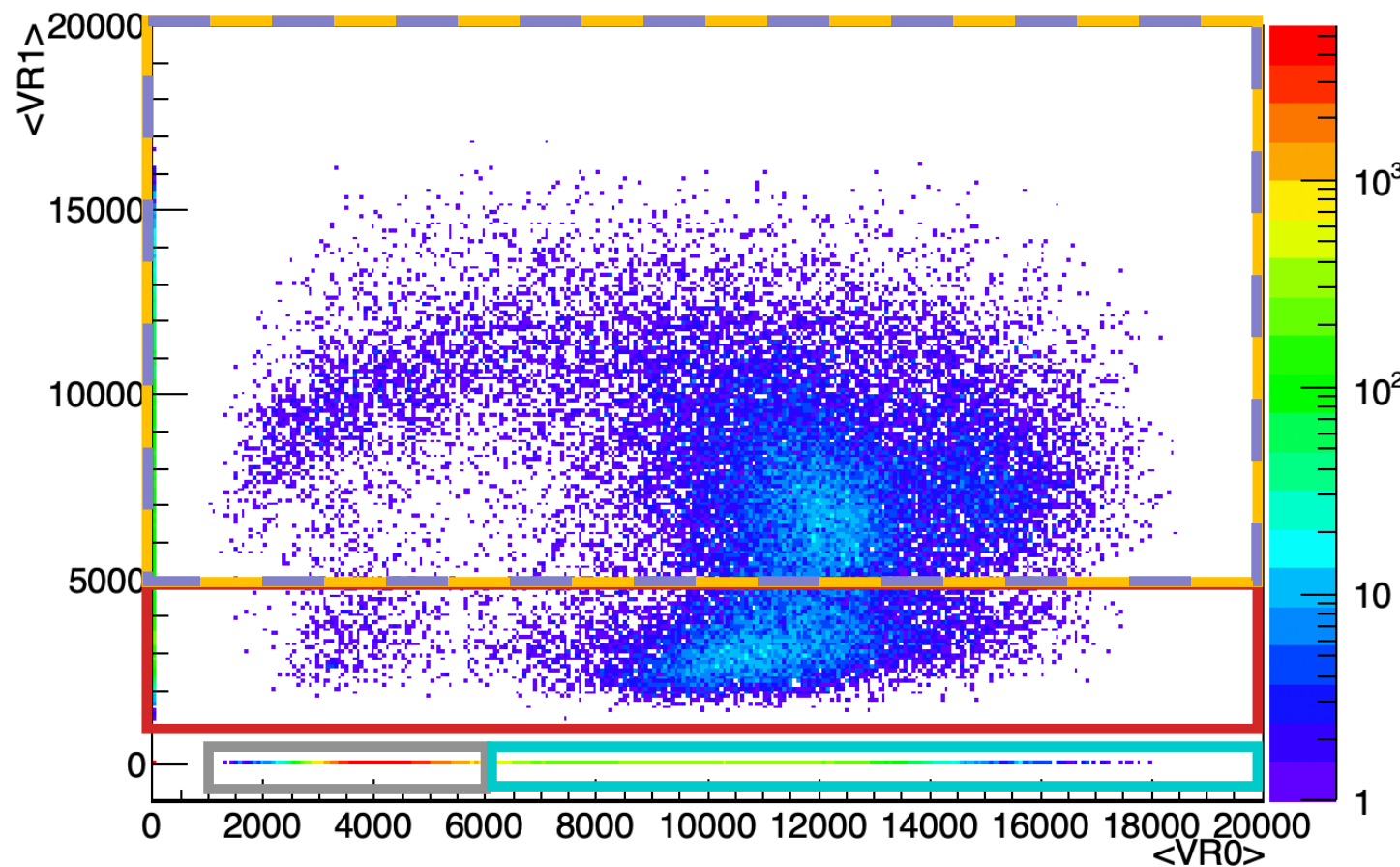


# Charge reconstruction - preliminary

- Charge analysis ongoing on GSI1-S2 data
- The charge assignment strategy works also on this dataset, as expected
- Results still preliminary



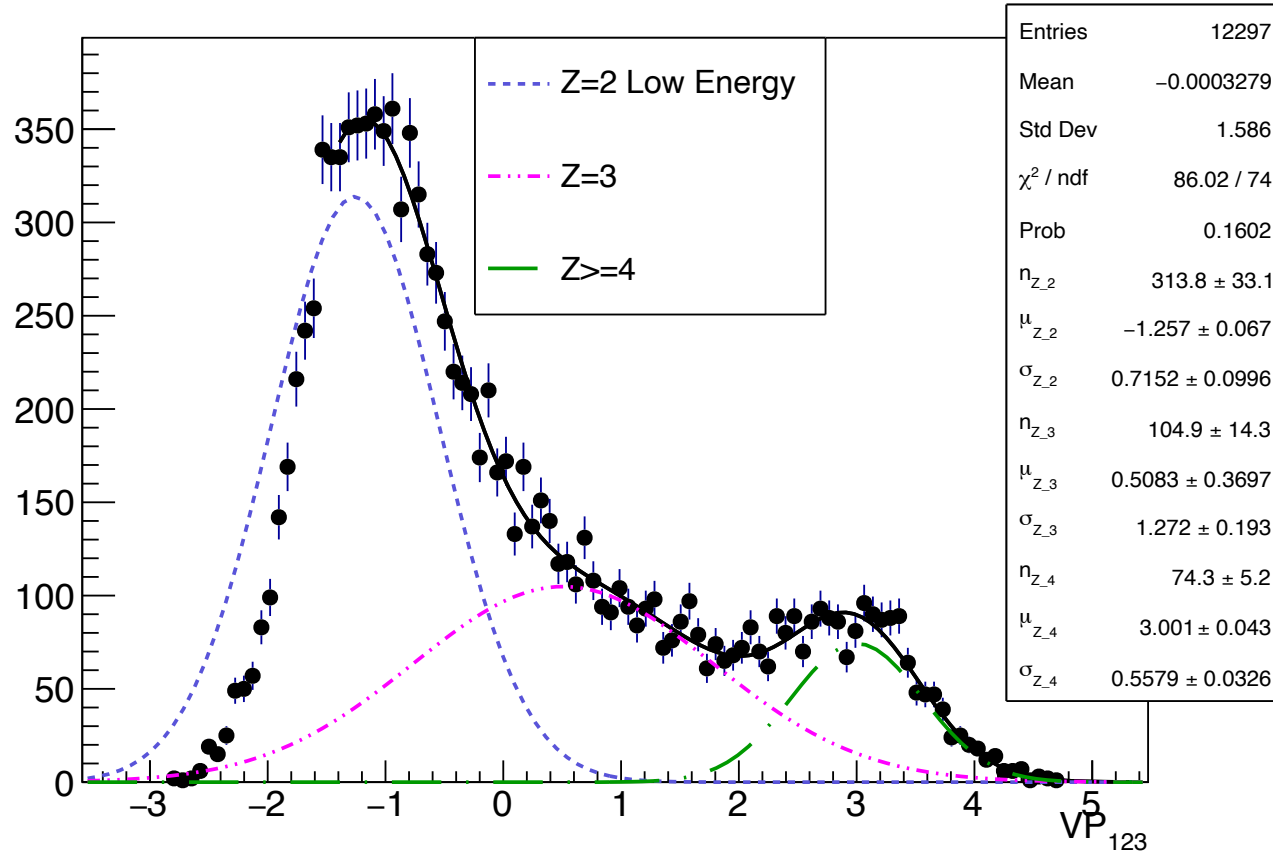
# Charge reconstruction - preliminary



- Cosmic Rays:  $0 < \langle VR0 \rangle < a\theta + b$  &  $nseg1 < 2$  &  $nseg2 < 2$  &  $nseg3 < 2$
- High energy Z=1:  $\langle VR0 \rangle \geq a\theta + b$  &  $nseg1 < 2$  &  $nseg2 < 2$  &  $nseg3 < 2$
- Low energy Z=1:  $\langle VR0 \rangle \geq 0$  &  $0 < \langle VR1 \rangle < c$  &  $nseg2 < 2$  &  $nseg3 < 2$
- High energy Z=2:  $\langle VR1 \rangle \geq c$  &  $nseg2 < 2$  &  $nseg3 < 2$
- Z $\geq 2$ : at least 3 VRx  $\rightarrow$  Principal Components Analysis



# Principal Component Analysis - Preliminary



- $VP_{123} = a \cdot \langle VR1 \rangle + b \cdot \langle VR2 \rangle + c \cdot \langle VR3 \rangle$
- 3 gaussian-model confirmed

# Conclusions

- The paper with charge assignment results will be submitted again in few days: all comments by referees have been answered
- GSI1 analysis started both on “reconstructed MC” and Data: quality checks ongoing before giving first results
- Still working to improve tracking and vertices reconstruction
- Charge analysis on GSI1 ongoing

**T**HANK **Y**OU!